Design and examination of a small-scale screw expander for waste heat recovery

M. Grieb, **A. Brümmer**
Chair of Fluidics, TU Dortmund University, Dortmund

Abstract

This paper first describes an exemplary design process for screw expanders in an exhaust heat recovery application where multi-chamber model simulation is simultaneously used with model scaling at constant circumferential speed to match expander size with Rankine cycle mass flow. The influence of geometric and cycle parameters on the operational behaviour of the screw machine and overall system efficiency are also discussed. Furthermore, expander specific design features are presented.

Within the scope of this investigation, an unsynchronised dry running screw expander prototype was built and evaluated on a steam test rig at TU Dortmund University. During the experimental investigation, a systematic variation of expander speed, inlet pressure, and steam overheating is carried out. The experimental results are presented and the influence of steam parameters on energy conversion within the expander is discussed. The characteristic map of the expander prototype is finally compared to multi-chamber model simulation results.

1. Introduction

Growing prices of primary energy carriers and increasing environmental requirements lead to the general need to enhance the efficiency of technical systems. A promising approach for both mobile and stationary applications containing internal combustion engines is exhaust heat recovery, where part of the waste heat flow is transferred to a coupled organic Rankine cycle in order to vaporise a pressurised working fluid, which in turn drives a heat engine. Previous investigations show that screw expanders offer a high potential for energy conversion in the lower and medium power range and therefore are highly suitable for heat recovery applications in closed-loop steam cycles [1] [2].

The crucial factor for achieving sufficient thermal efficiency of the recovery system is expander net power [3]. It can be influenced by choosing the right screw expander geometry as well as by operating the Rankine cycle at an advantageous operation point [4]. For optimal results during the design process, an integral approach should be favoured over expander-based optimisation. This paper contains a brief description of an exemplary

application-oriented design for a screw-type expander (ethanol vapour driven) for exhaust heat recovery of heavy truck engines. The design procedure is performed with ethanol as the ORC working fluid since it has advantageous properties for this specific case of application [5]. Furthermore, a theoretical investigation of the expander's operational behaviour is carried out and compared to experimental results taken from an actual examination conducted on a steam test rig.

2. Fundamentals

2.1. Screw expanders

Screw expanders are two-shaft rotary positive displacement machines with a defined expansion ratio. The characteristic rotor pair is made up of two matching helical screws that are constantly meshed during operation. As the profiled rotor parts are enclosed in a tight housing, working chambers, connected in pairs, form between the screw lobes and periodically change their volume as the rotors rotate. Chamber filling and working fluid discharge is controlled by the position of inlet and outlet openings within the casing.

Figure 1 shows chamber volume progression as well as the inlet and outlet openings in the screw-type expander examined during its working cycle. A new chamber emerges between the lobes on the high pressure side of the expander while the rotors turn in opposite directions. It is connected to the expander inlet port so that working fluid flows in while chamber volume increases. The position of the high pressure control edge defines the angular position of the rotor as well as the corresponding chamber volume $V_{ex,th}$ when the filling process stops and the subsequent expansion phase begins. Chamber volume continuously increases during expansion while the chamber in question is ideally isolated from its environment. Thus chamber pressure drops. The leading lobes cross the low pressure control edge of the casing when maximum chamber volume V_{max} is reached and the discharge phase begins. At this point fluid contained is displaced to the expander outlet while chamber volume simultaneously decreases. Since screw machines operate without dead spaces, the working cycle ends when the chamber in question disappears. Given that the angular position at maximum chamber volume is affected by screw rotor geometry, the angular position of expansion initiation depends on the inner volume ratio v_i, defined in the following equation (1).

$$v_i = \frac{V_{max}}{V_{ex,th}} \tag{1}$$

The expander's inner volume ratio is a crucial parameter because it defines the screw expander's inner expansion. A large inner volume ratio leads to a shorter filling time and thus to a smaller cross section of the inlet opening. As a result, throttling effects increase when filling the chamber. Another effect that impacts working behaviour is inevitable leakage through clearances required to separate moving parts from each other and from the casing. This can be reduced however by injecting an auxiliary liquid into the working chamber in order to seal clearances.

Like all positive displacement machines, screw expanders change the energy content of a working fluid by performing pressure-volume work, which is finally converted to shaft work. Effective isentropic efficiency $\eta_{e,s}$ is hence defined as shown in equation (2), where M is the torque obtained from the shaft and ω is the angular velocity. The available isentropic power P_s can be determined through knowing the expander mass flow rate $\dot{m}$ and the isentropic enthalpy difference, where $h_{out,s}$ represents the specific enthalpy after an isentropic expansion to expander back pressure. h_{in} is determined by expander inlet pressure and inlet temperature.

$$\eta_{e,s} = \frac{P_e}{P_s} = \frac{M\,\omega}{P_s} = \frac{M\,\omega}{\dot{m}\left(h_{in} - h_{out,s}\right)} \tag{2}$$

The definition of thermal efficiency η_{th} for the Rankine cycle is given in equation (3), where $\dot{Q}_{exh}$ represents the exhaust gas heat flow and P_{ORC} the recovered net power, which is composed of effective expander power P_e and power consumption of the feed pump P_{pump}.
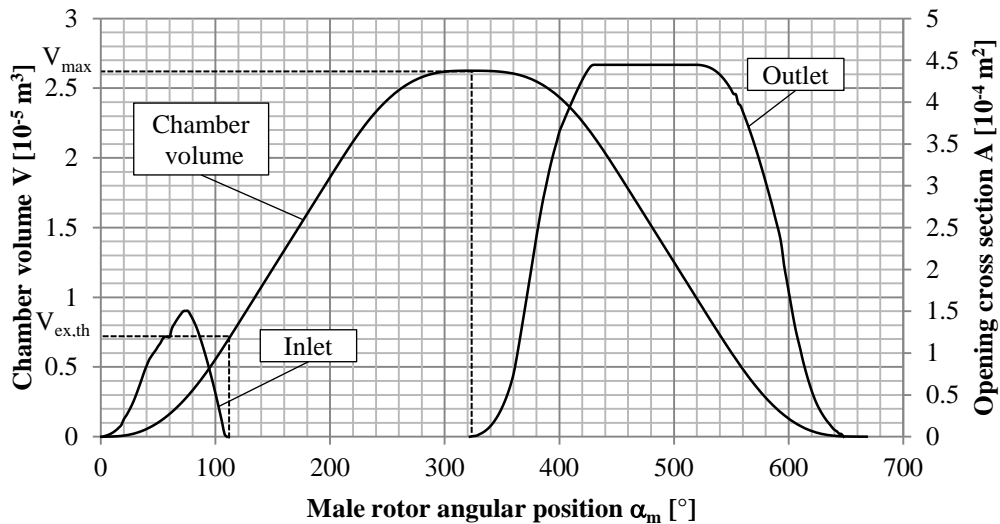
Fig. 1: Volume curve and chamber openings of the examined screw expander for a working cycle.

$$\eta_{th} = \frac{P_{ORC}}{\dot{Q}_{exh}} = \frac{|P_e| - P_{pump}}{\dot{Q}_{exh}} \qquad (3)$$

The delivery rate λ defined in equation (4) is a measurement of expander mass flow. $\dot{m}_{th}$ is the theoretical mass flow, which would occur in the case of lossless chamber filling without internal leakage, meaning that fluid density at expansion start would correspond to inlet conditions ρ_{in}. Inlet throttling reduces the delivery rate since the actual density at the beginning of expansion is lower than the density in the inlet. Internal leakage on the other hand increases the delivery rate because leakage mass flows are directed in the same direction as the main flow.

$$\lambda = \frac{\dot{m}}{\dot{m}_{th}} = \frac{\dot{m}}{V_{ex,th}\ \rho_{in}\ z_m\ \omega_m/2\ \pi} \qquad (4)$$

Theoretical power P_{sv} is determined for an idealised working process (with idealised pressure history) of a screw expander with isobaric charge and discharge phases, isentropic expansion corresponding to the inner volume ratio, and isochoric adaption to outlet pressure, equation (5). Delivery rate for the idealised process is 1.0.

$$P_{sv} = \dot{m}_{th}\ \left(h_{in} - h_{dis,s,th} + v_i\ v_{in}(p_{dis,s,th} - p_{out})\right) \qquad (5)$$

Further expander parameters describing the screw geometry are listed below:
- Rotor profile
- Number of lobes z_m, z_f
- Length diameter ratio of male rotor L_m/D_m
- Wrap angle of male rotor φ_m

These geometric design parameters and the choice of inner volume ratio affect the operating behaviour of screw expanders as they not only specify the size and position of chamber openings, and thus the magnitude of inner expansion, but also define the clearance geometry and, thus, any internal leakage.

2.2. Multi-chamber simulation

Multi-chamber simulation is used to predict the operating behaviour of the screw expander where the screw machine is abstracted to a zero-dimensional time-dependent model, which includes all relevant information. The universal positive displacement machine simulation tool KaSim utilised in this investigation was developed by the Chair of Fluidics at TU Dortmund University. All chambers, chamber connections, and miscellaneous capacities are observed simultaneously during thermodynamic simulation. The exchange of mass and energy

between chambers or expander ports is considered as well as changes of state through volume alteration. The laws of mass and energy conservation serve as the basis for calculation. Simulation results are, on the one hand, integral values such as expander mass flow or internal power, and on the other hand time-dependent pressure and temperature diagrams. [6] [7]

Designing a screw expander for a closed-loop application requires adapting expander behaviour to the ORC since the two components are highly dependent on each other. Steady operation is only possible if the expansion device delivers the evaporated vapour flow for the specified system parameters, such as inlet pressure and degree of superheating. Moreover, expander circumferential speed for the design point is chosen according to whether a dry running or a liquid-injected screw machine is considered. Thus, machine size has to be iteratively adapted during simulation to obtain the intended mass flow with the given circumferential speed. In the design calculations ethanol vapour is used as the working fluid, a clearance height of 0.1 mm and a male rotor circumferential speed of 35 m s^{-1} (for an liquid-injected machine) are determined and reduced flow coefficients for internal clearances are set in order to consider the seal through auxiliary liquid. [8]

The flow coefficient α is defined as quotient of an actual mass flow $\dot{m}$ (through a clearance or machine part cross section) and the theoretical mass flow $\dot{m}_{th}$ for the available pressure ratio, equation (6).

$$\alpha = \frac{\dot{m}}{\dot{m}_{th}}$$
(6)

Simulations with steam and an adiabatic model are performed to make a comparison to experimental results from the test rig. Vapour is initially implemented as monophasic fluid in KaSim meaning that slightly wet vapour is still treated as saturated vapour.

3. Integral design approach

Screw machines are traditionally designed by focusing on the thermodynamic machine itself. Most often, geometric parameters and expander size are optimised based on a defined set of boundary conditions that reflect actual application conditions (e.g. mass flow rate, pressure levels, and temperatures). An optimisation in terms of expander net power output would therefore equate to maximising isentropic efficiency of the expansion device since the available isentropic power is inevitably defined by the application boundary conditions. The screw expander looked at in this paper is designed with an application-oriented approach, where expander parameters are optimised along with system parameters to exploit the whole system's potential. Hence the available exhaust gas heat flow is the main boundary condition

in this expander's design process. Given that available isentropic power depends on Rankine cycle operation and is therefore variable, the integral optimisation in terms of expander power output equates to maximising the thermal efficiency of the heat recovery system.

Featuring variations in expander geometry and ORC parameters, this application-oriented design approach to screw expanders for exhaust heat recovery in heavy truck engines leads to the following findings. On a theoretical base, best results are achieved with ethanol as the working fluid when expander inlet pressure is set to $50 \cdot 10^5$ Pa for saturated vapour. The ORC mass flow rate only moderately depends on the expander inlet pressure and decreases in tandem with the degree of overheating. However, available isentropic power considerably decreases along with expander inlet pressure. Since such high pressure ratios obviously cannot be entirely relaxed in a one-staged screw expander, isentropic efficiency ratings decrease with high inlet pressures. Despite that, the highest thermal efficiency is achieved with an expander inlet pressure of $50 \cdot 10^5$ Pa and a screw expander with an uncommonly large internal volume ratio of $v_i = 8$. [8]

4. Design of the prototype expander

The application-oriented design approach leads to a small-scale screw expander featuring significant differences compared to traditionally-designed screw machines. The high inner volume ratio and intended operation with pressure ratios of up to 50 are especially unique. Geometric parameters such as length to diameter ratio, inner volume ratio, and the number of lobes are varied systematically. Five operation points of the internal combustion engine are considered and used to average the expander's final size. The geometric parameters of the screw expander in question are displayed in **Table 1**.

An oil-flooded machine is chosen for the ORC application in order to reduce system complexity. The oil is mixed with the working fluid and flows through the closed-loop cycle, meaning it enters the expander through the inlet opening. The purpose of the oil is to

Table 1: Geometry parameters of the final expander design.

Profile	SRM "A"
Number of lobes	$z_m = 4$; $z_f = 6$
Length to diameter ratio	$L_m/D_m = 1.0$
Male rotor wrap angle	$\varphi_m = 200°$
Inner volume ratio	$v_i = 8.0$ (4.0 for steam test rig)
Rotor center distance	46.2 mm
Maximum chamber volume	$V_{max} = 26254$ mm^3

lubricate the unsynchronised pair of rotors and roller bearings as well as reducing internal leakages by sealing part of the clearance cross sections. Choosing a high inner volume ratio automatically leads to a relatively small axial inlet opening. However, the inlet flange is placed on the top side of the expander and the inlet flow is directed within the casing. Both axial and radial outlet openings are positioned in the housing. PTFE O-rings and a magnetic coupling transmitting the torque provide a hermetic seal, which is a major requirement for expanders in closed-loop applications. A segmental construction found in the prototype allows for modification of the inner volume ratio. Furthermore, a variation of clearance heights is accomplished by adapted rotor pairs and distance sleeves that adjust the axial bearing position on the shafts.

The expander's initial experimental investigation is carried out on a steam test rig. To adapt the expansion ratio to the available pressure ratio of the test rig, a configuration with an inner volume ratio of 4.0 is selected. The expander is equipped with sealed high precision roller bearings lubricated with grease since no oil is supplied. Bores in the casing channel condensed liquid to the machine outlet so as to protect the bearings from corrosion. To enable test operation of the unsynchronised screw expander without lubricating the profile mesh, the profile surfaces are case-hardened and hard-coated with a DLC layer.
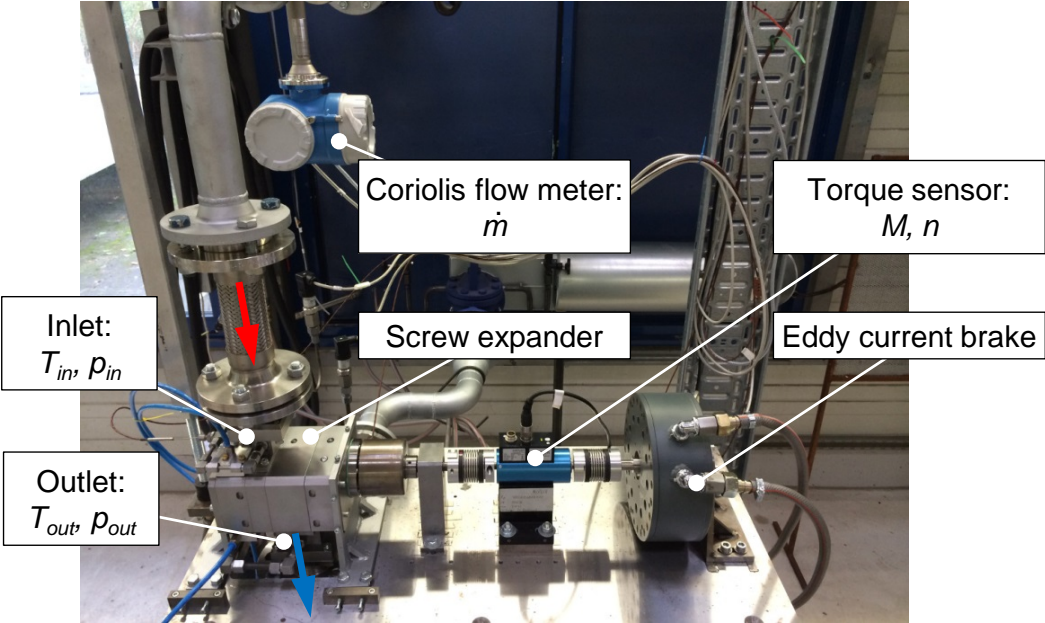
Fig. 2: Screw expander mounted on steam test rig.

5. Experimental investigation and comparison with multi-chamber simulation

5.1. Test rig

Figure 2 shows the screw expander and all relevant measurement points on the steam test rig. Mass flow rate is directly measured with a coriolis flow meter on the high pressure side. Pressure and temperature levels are metered in the inlet and outlet port of the screw expander. Expander speed and the torque obtained from the male rotor shaft are measured with a torque sensor. An eddy current brake with a controller is utilised to hold the settings for expander speed constant. The steam is produced in a gas-powered boiler. An additional electric heat exchanger allows moderate superheating of the steam. Expander inlet pressure is regulated with a motor operated valve in a bypass. Initial experiments are carried out with a constant back pressure corresponding to ambient conditions. A maximum mass flow rate of 0.1 kg s^{-1} can be realised at a maximum pressure of $12 \cdot 10^5$ Pa.

Unfortunately, the first setup of the screw expander on the test rig caused distinct vibrations. An imbalance of the outer coupling magnet mounted in a cantilever position induced vibrations at rotary frequency. Safe operation was only ensured in the lower speed range since vibration velocity values significantly increased. Only moderate values of efficiency and power could hence be achieved in the scope of this investigation. A more precise balancing of the coupling and modifications of the bearing system are necessary to obtain test data at higher expander speeds. Even though it leads to large internal leakage and thus poor efficiency, a clearance height of 0.2 mm is chosen for initial testing to avoid damage from thermal elongation.
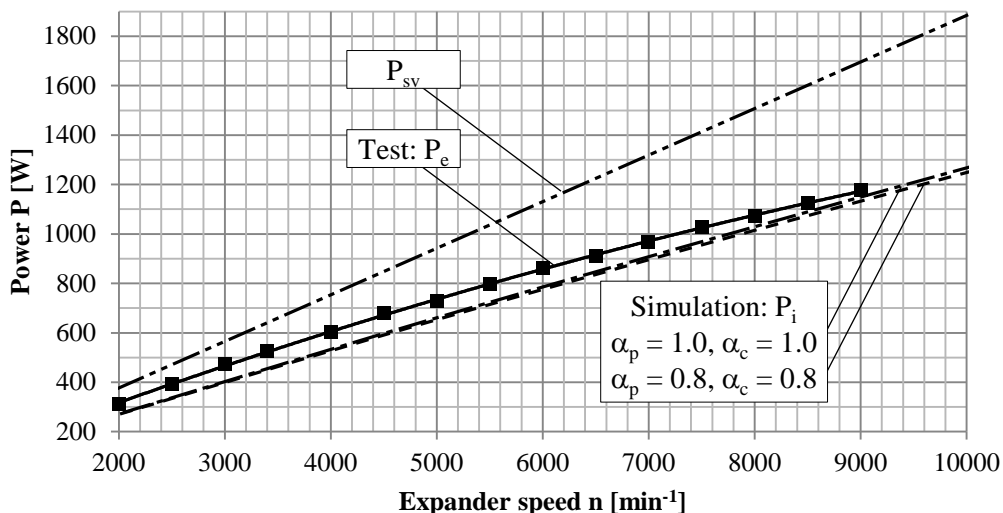
Fig. 3: Effective power (experiment), inner power (simulation) and theoretical power as a function of expander speed; $p_{in} = 4 \cdot 10^5$ Pa, wet steam.

5.2. Influences of wet steam on screw expander operation

First test runs are carried out without overheating the steam. As a consequence, an undefined amount of liquid water is fed to the expander together with the steam flow. The liquid fluid originates in condensation in the piping as well as the steam flow entraining water droplets from the boiler. A comparison of measurement results and multi-chamber simulations is given in **figure 3**. Additionally, values of theoretical power representing an ideal working cycle of the expander in question are displayed (isobaric inlet and outlet phase, isentropic inner expansion, isochoric adaption to back pressure). All simulation flow coefficients for internal clearances α_c and machine ports α_p are set to 0.8 and 1.0, respectively. During calculation neither a liquid phase is taken into account nor mechanical energy loss due to fluid and mechanical friction.

In the speed range examined, the effective power of the screw expander is greater than the inner power calculated with integral flow coefficients of 0.8 or even 1.0. The achieved inner power of the test machine thus has to be even greater. Since power of positive displacement machines mainly depends on the gaseous working fluid's pressure history during the working cycle, it can be assumed that the average pressure within the working chambers for the prototype machine exaggerates that calculated during simulation. An overall variation of flow coefficients only slightly affects inner power values, and hence mean chamber pressure. The deviation in power output could therefore be explained by reduced internal leakage in combination with adequate chamber filling. The power gradient decreases at higher expander speeds while simulation shows a linear progression. The expected substantial
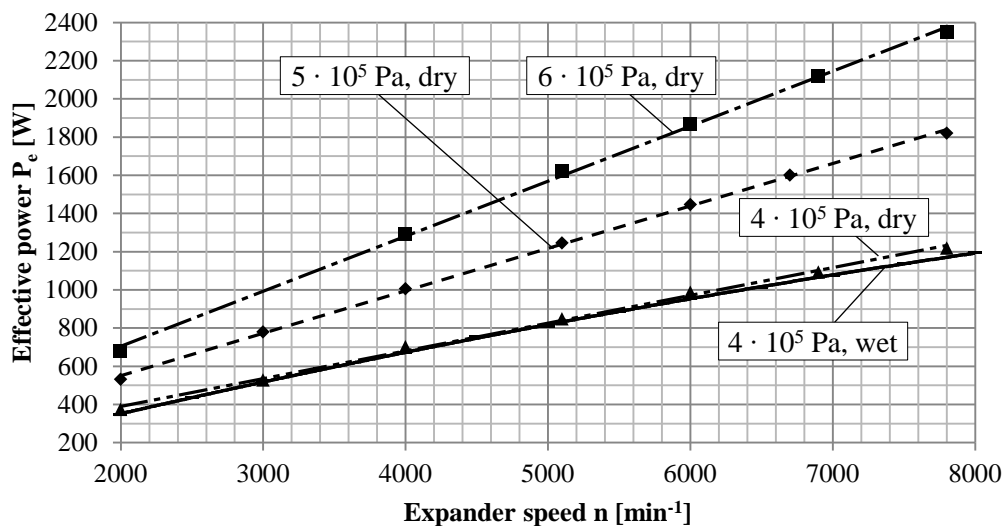
Fig. 4: Effective power (experiment) as a function of expander speed; $p_{in} = 4 \ldots 6 \cdot 10^5$ Pa, 10 K superheating; $p_{in} = 4 \cdot 10^5$ Pa, wet steam.

reason for this deviation is the speed-dependent increase of fluid and mechanical friction within the expander. Since density of the two-phase mixture is raised, the liquid phase in the inlet flow does not only affect power output but also the delivered mass flow rate. Furthermore, the unsteady partial flow of liquid water affects metering of the mass flow rate with the coriolis flow meter. The liquid, being clearly visible in a sight glass before entering the flow meter, leads to relatively large measurement inaccuracy. However, mean mass flow values are located between simulation results for $\alpha = 1.0$ and $\alpha = 0.8$. Taking into account the fact that a notable amount of liquid water not considered in the simulation is fed to the expander in the experiment, it can be assumed that vaporous flow is noticeably lower than the figures calculated in multi-chamber simulations. Again, this indicates reduced internal leakage probably caused by liquid water within the screw expander.

To avoid measurement inaccuracy caused by the liquid, and to preserve accurately defined inlet conditions (since the amount of water cannot be determined), further investigations are carried out with superheated steam.

5.3. Experimental investigation with superheated steam

Test results for effective power are displayed in **figure 4**. For the speed range in question, the coherence between expander speed and power output is almost linear. A maximum in power output cannot be achieved within the limited speed range. Consequently, a further increase of effective power is expected for higher expander speeds. Compared to operation with wet steam, decreasing gradients are less distinct for superheated steam. Fluid friction of
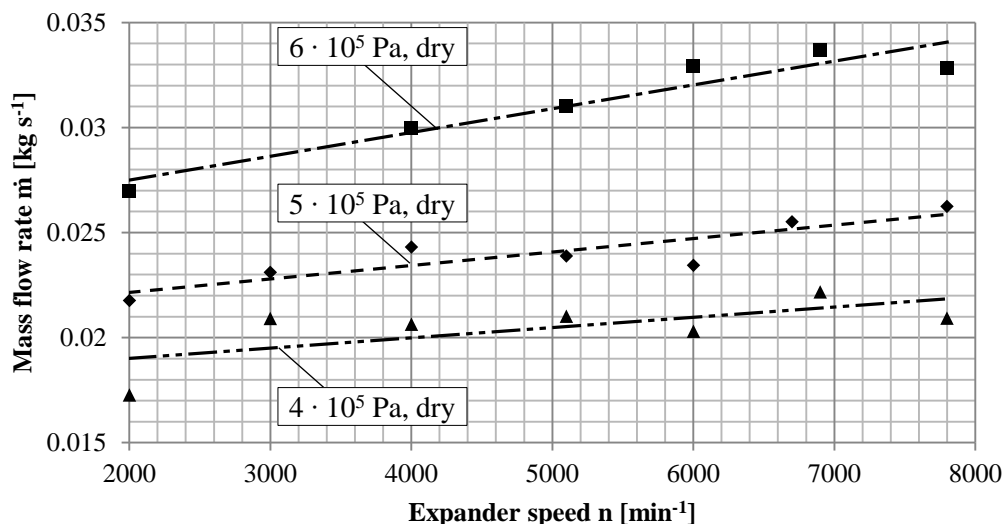
Fig. 5: Mass flow rate (experiment) as a function of expander speed; $p_{in} = 4 \dots 6 \cdot 10^5$ Pa, 10 K superheating.

liquid water thus seems to have an inferior impact and, as a consequence, greater power output is generated than in operation with wet steam. The mass flow rate only slightly increases with expander speed (**figure 5**), which is primarily due to expander operation being highly influenced by internal leakage at low rotational speed. As a result of large clearance heights, absolute delivery rate values for these operation points are greater than 3.04, leading inevitably to poor isentropic efficiency (lower than 24.07 %). A distinctly enhanced efficiency is expected with a reduction of clearance height and operation at higher speeds. However, the achieved effective power of the test machine again significantly exaggerates multi-chamber simulation results with conventional flow coefficients of 0.8 for clearance connections and chamber ports. This again implies pressure history within the test machine being higher than calculated. The experimentally determined mass flow rate also lies above first multi-chamber simulation results, which leads to a contradiction between model and experiment.

For an adiabatic model with a monophasic working fluid, simulation pressure history, and thus power output, can only be raised by increasing the amount of vapour enclosed in the working chamber (i.e. by increasing flow coefficients for the inlet port) or by decreasing internal leakage (i.e. by decreasing flow coefficients for clearance flows). For a detailed comparison, the port flow coefficient is set to 1.0 and coefficients for clearances are reduced systematically, **figure 6**. Even though clearance flows are reduced by up to 40 % of their theoretical value for simulation, an effective power still higher than the calculated inner power is obtained from the experiment in lower speed ranges. With the boundary condition of a
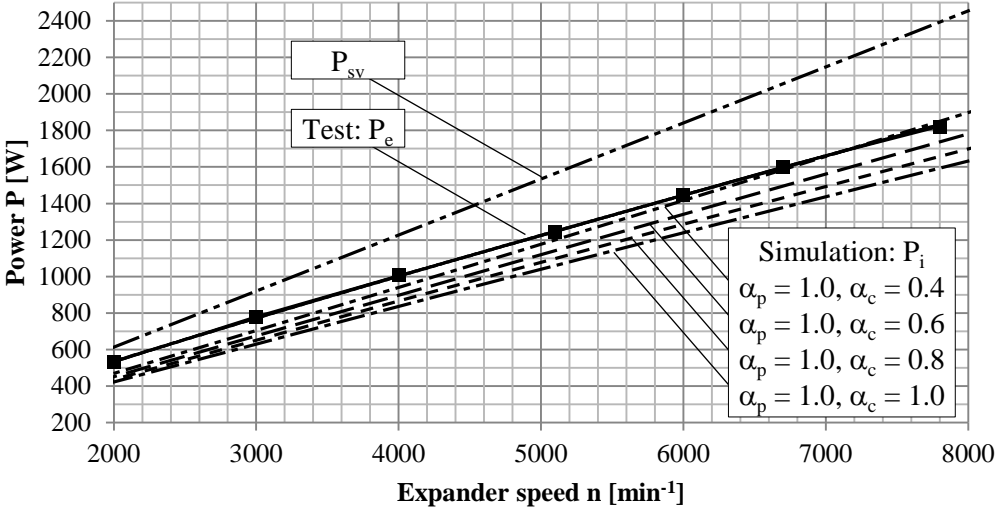
Fig. 6: Comparison of effective power (test), theoretical power and inner power for various clearance coefficients (simulation); $p_{in} = 5 \cdot 10^5$ Pa, 10 K superheating.
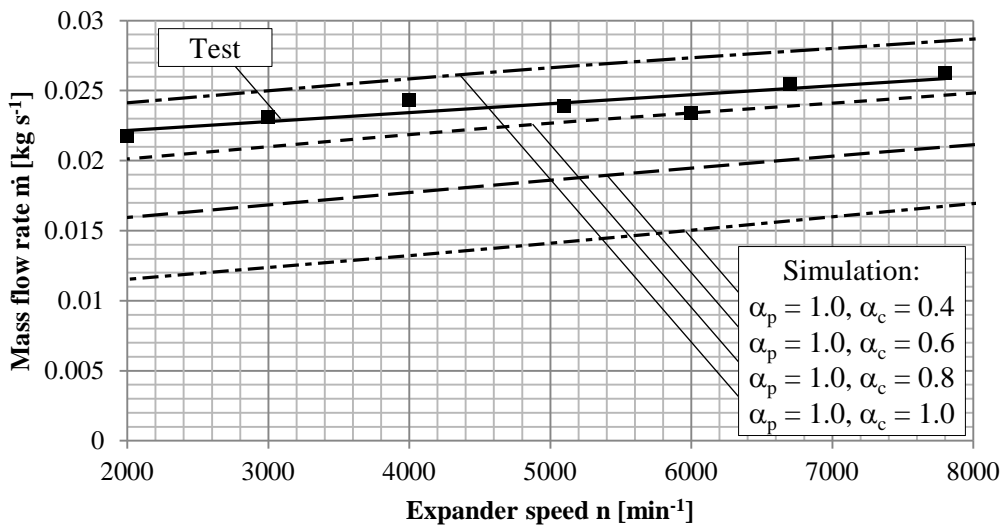
Fig. 7: Comparison of mass flow rates between experimental obtained data and simulation results for various clearance coefficients; $p_{in} = 5 \cdot 10^5$ Pa, 10 K superheating.

single phase vapour expansion, this is only explainable by a massive reduction of internal leakage, which inevitably causes a drop in expander mass flow, **figure 7**. Mass flow rates from experimentation and simulation obviously do not correspond when a reduced internal leakage is modelled. However, the mass flow curves show a rather good accordance between gradients.

These results indicate a physical mechanism that affects the operation of the screw expander which is not considered in multi-chamber simulations carried out. Vapour was initially implemented in KaSim as monophasic fluid, meaning that no phase transition is calculated. This was performed in light of an estimate that the wet steam region is only accessible at steam qualities greater than 90 % for realistic isentropic efficiency. Apparently, changes of state of the vaporous working fluid are more complex; an improvement of the model might be necessary for a more adequate prediction of screw expander operation with steam.

There are various physical effects that could theoretically lead to the deviation between experiment and simulation. Condensation on machine parts during the inlet phase, for one thing, would cause a decrease in specific volume and thus a greater mass being displaced per working cycle. Liquid water would additionally effect a partial seal of internal clearances. Further condensation during expansion, for another thing, would cause a pressure drop in the enclosed working chambers, which would be contradictory to obtained power data. But

then again, hypothetically speaking, condensate emerging at high pressure could re-evaporate (and therefore perform pressure-volume work) when pressure is rapidly decreased during the expansion phase. Another potential reason for reduced leakage and therefore higher pressure history could be the reduced speed of sound in chocked two-phase flows through clearances. Further investigation is needed to verify in which way these phenomena affect operation of steam-driven screw expanders. A first step would be to record pressure history during expansion to obtain a detailed understanding of the inner work of the screw expander in question.

6. Conclusion

In this paper, an integral design approach for the design of screw expanders for closed-loop cycles is presented. It becomes apparent that system parameters (e.g. pressure and temperature levels) should be varied with expander geometry in order to find a beneficial combination that maximises the application's thermal efficiency. Furthermore, design features of a small-scale screw expander for exhaust heat recovery of heavy truck engines are introduced. Initial testing of the screw expander is carried out on a steam test rig and the data obtained is presented and finally compared to multi-chamber simulation results. Greater power output is generated on the test rig than in the simulation, which is potentially caused by the phase transition of water during expansion. Further investigations are in progress to verify these assumptions.

Nomenclature

A	Cross section	$[m^2]$	v	Specific volume	$[m^3\ kg^{-1}]$
h	Specific enthalpy	$[J\ kg^{-1}]$	v_i	Inner volume ratio	$[-]$
D	Diameter	$[m]$	V	Volume	$[m^3]$
L	Length	$[m]$	z	Number of lobes	$[-]$
$\dot{m}$	Mass flow rate	$[kg\ s^{-1}]$	α	Angular position	$[°]$
M	Torque	$[N\ m]$	α	Flow coefficient	$[-]$
n	Rotational speed	$[min^{-1}]$	η	Efficiency factor	$[-]$
ORC	Organic Rankine cycle	$[-]$	λ	Delivery rate	$[-]$
p	Pressure	$[Pa]$	ρ	Density	$[kg\ m^{-3}]$
P	Power	$[W]$	φ	Wrap angle	$[°]$
$\dot{Q}$	Heat flow	$[W]$	ω	Angular velocity	$[s^{-1}]$
T	Temperature	$[K]$			

Subscript

c	Clearance	m	Male
dis	Discharge	max	Maximal
e	Effective	out	Outlet
ex	Expansion	p	Port
exh	Exhaust	s	Isentropic
f	Female	th	Thermal
i	Inner	th	Theoretic
in	Inlet	v	Isochoric

References

[1] Hütker, J., Brümmer, A.: Physics of a dry running unsynchronized twin screw expander. 8th International Conference on Compressors and their Systems, Woodhead Publishing, London, 2013, p. 407-416

[2] Smith, I. K., Stosic, N., Kovacevic, A.: Power recovery from low-grade heat by means of screw expanders. Woodhead Publishing, 2014

[3] Brümmer, A.: Energieeffizienz – Abwärmenutzung durch Schraubenexpander. Pumpen, Kompressoren und prozesstechnische Komponenten, 2012, p. 120-126

[4] Hütker, J., Brümmer, A.: A comparative examination of steam-powered screw motors for specific installation conditions. 8. VDI-Fachtagung Schraubenmaschinen 2010, VDI Bericht 2101, 2010, p. 109-123

[5] Span, R., Eifler, W., Struzyna, R.: Nutzung der Motorabwärme durch Kreisprozesse, Informationstagung Motoren/Turbomaschinen, Heft R553, FVV, Bad Neuenahr, 2011

[6] Peveling, F.-J.: Ein Beitrag zur Optimierung adiabater Schraubenmaschinen in Simulationsrechnungen. Dissertation, Universität Dortmund, 1987

[7] Janicki, M.: Modellierung und Simulation von Rotationsverdrängermaschinen. Dissertation, Universität Dortmund, 2007

[8] Grieb. M., Brümmer, A.: Application-Oriented Design and Theoretical Investigation of a Screw-Type Steam Expander. Proceedings of the International Compressor Engineering Conference at Purdue, 2014